ISSN 2072-5981
doi: 10.26907/mrsej

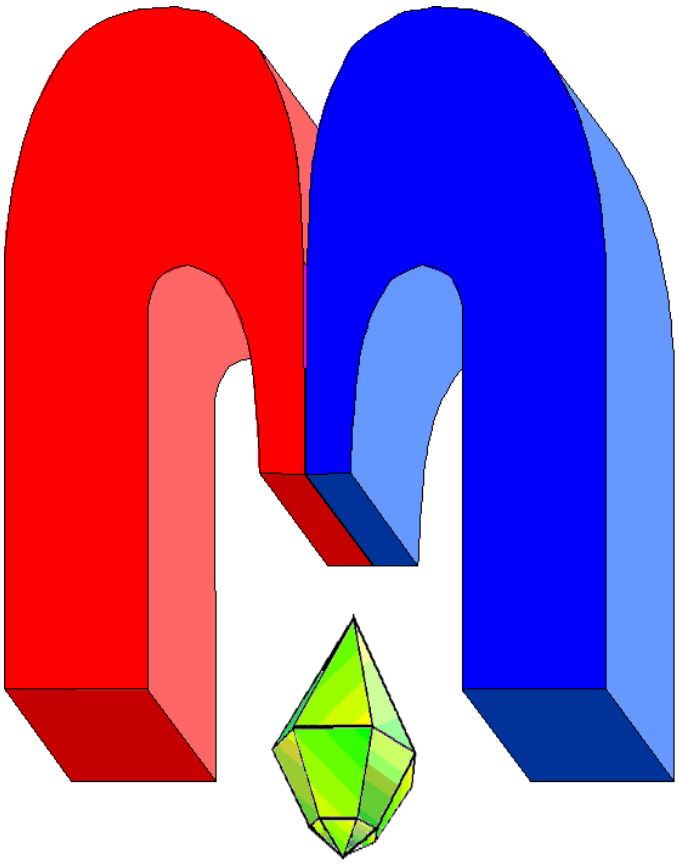

Magnetic Resonance in Solids

Electronic Journal

Volume 27
Issue 3
Article No ***25309***
1-10 pages
2025
doi: **10.26907/mrsej-25309**

http://mrsej.kpfu.ru
http://mrsej.ksu.ru
http://mrsej.elpub.ru

Established and published by Kazan University*
Endorsed by International Society of Magnetic Resonance (ISMAR)
Registered by Russian Federation Committee on Press (#015140), August 2, 1996
First Issue appeared on July 25, 1997

"***Magnetic Resonance in Solids. Electronic Journal***" (**MRS*ej***) is a peer-reviewed, all electronic journal, publishing articles which meet the highest standards of scientific quality in the field of basic research of a magnetic resonance in solids and related phenomena.

Indexed and abstracted by
Web of Science (*ESCI*, Clarivate Analytics, from 2015), *Scopus* (Elsevier, from 2012), *RusIndexSC* (*eLibrary*, from 2006), *Google Scholar*, *DOAJ*, *ROAD*, *CyberLeninka* (from 2006), *SCImago Journal & Country Rank*, etc.

Guest Editor‡: *Marat Gafurov (KFU, Kazan)*

---

* Address: "Magnetic Resonance in Solids. Electronic Journal", Kazan Federal University; Kremlevskaya str., 18; Kazan 420008, Russia

† In Kazan University the Electron Paramagnetic Resonance (EPR) was discovered by Zavoisky E.K. in 1944.

‡ This paper was selected at the International Conference "Modern Development of Magnetic Resonance 2025", September 29 -- October 3, 2025, Kazan, Russia.

Low-field ^{129}Xe NMR of liquid Xenon near the triple point: experimental design, relaxation measurements, and preliminary applications to porous media†

K.O. Sannikov*, A.V. Klochkov

Institute of Physics, Kazan Federal University, Kazan 420008, Russia

**E-mail: KirOSannikov@kpfu.ru*

(received October 22, 2025; revised December 22, 2025; accepted December 23, 2025; published December 29, 2025)

In this article, the capabilities of using low-field NMR of liquid ^{129}Xe near triple point in the study of porous media were demonstrated. The possibility of detecting the NMR signal of Xenon with natural isotopic composition and Boltzmann equilibrium spin polarization in the liquid and solid phases was explored. The problems encountered during the planning and conducting the experiments, along with their solutions, are presented. Key issues included low sensitivity, particularly in magnetic fields up to 1 T; difficulties in filling the experimental cell with liquid Xenon; the critical need to control the temperature gradient along the NMR probe axis and prevent capillary blockage; control of the solid-to-liquid transition; RF-noise from the electrical leads. As a result, spin-lattice relaxation times (T_1) of bulk Xenon were measured and the spin-spin relaxation times (T_2) of bulk Xenon were estimated. Some of preliminary results on ^{129}Xe NMR in porous media are presented.

PACS: 76.60.-k, 81.05.Rm, 81.70.-q, 07.05.Fb.
Keywords: NMR, Xenon, ^{129}Xe, low temperatures, porous media, phase transition.

1. Introduction

The development and study of new nanostructured and nanoporous materials require various control and characterization methods. Nuclear magnetic resonance (NMR) porosimetry using inert gases such as Xenon and ^{3}He at low temperatures presents a promising alternative to classical porosimetry techniques. Xenon and ^{3}He are inert gases, so their use is non-destructive to samples and their surfaces, and these elements are absent in the samples prior to experiment. Natural Xenon consists of seven stable isotopes. ^{129}Xe is particularly suitable for NMR applications due to its relatively high natural abundance (NA = 26.4%) and a nuclear spin of $I = 1/2$. With its 54 electrons, Xenon possesses a large, highly polarizable electron cloud, making it extremely sensitive to the surrounding environment [1].

A method for investigating porous media using ^{3}He NMR has been developed and tested at low temperatures on various samples, including aerogels [2], nanodiamonds [3], and geological samples [4]. This method enables the evaluation of sample porosity, the depth of paramagnetic impurities in the surface layer of nanoparticles, and other parameters. ^{3}He, with the smallest kinetic diameter (0.25 nm) among of all molecules, can access the smallest pores, thereby allowing the determination of true porosity, which is often inaccessible by other techniques. Information on the pore size distribution can be derived from the analysis of ^{3}He spectra and NMR relaxometry. The relaxation times T_1 and T_2 of ^{3}He depend on the surface-to-volume ratio of the pores due to effective surface relaxation, while the integrated porosity is determined by the amplitude of the ^{3}He NMR signal within the sample pores [5].

†This paper was selected at the International Conference "Modern Development of Magnetic Resonance 2025", September 29 – October 3, 2025, Kazan, Russia. The guest Editor, Prof. M.R. Gafurov, was responsible for the publication, which was reviewed according to the standard MRSej procedure.

The first NMR experiments with ^{129}Xe were conducted in 1950–1951 when Proctor and Yu reported the magnetic moment of this isotope [6, 7]. The initial development of Xenon NMR for porous media studies began in the 1980s with investigations of zeolite pore structures. It was found that the chemical shift of Xenon adsorbed in zeolites is highly sensitive to both cavity size and the presence of impurities on the surface [8]. Following the production of hyperpolarized Xe in 1991 [9], the method has been widely employed for studying various nano- and microstructures, where the chemical shift serves as the primary source of information about pore space properties. To date, numerous studies and reviews have been published on the use of Xenon as a probe for investigating the properties of diverse structures, biological systems, and geological objects [1, 10, 11]. Nevertheless, low-field NMR of Xenon is a more cost-effective method compared to high-field NMR, as well as using of Boltzmann polarized Xenon is technically simpler.

While hyperpolarization techniques can significantly enhance the Xenon NMR signal, the study of Xenon in its thermal equilibrium (Boltzmann-polarized) state is still an interesting subject for fundamental physics. Notably, less attention has been paid to the properties of ^{129}Xe near the triple point. Xenon with equilibrium polarization provides a stable system for probing material properties and interactions, free from the experimental complexities and potential systematic effects associated with external polarization methods. The key advantages lie in its long-term stability, controllability, and the absence of polarizing agents, making it an ideal probe for high-precision measurements. This is especially important in porous media research, where Xenon with Boltzmann polarization serves as a versatile probe for investigating pore structures, nanoscale magnetism, and other surface characteristics. Despite its larger kinetic diameter (0.405 nm [13]) compared to ^{3}He, a significant advantage of ^{129}Xe is the possibility of using liquid nitrogen as a coolant in a flow cryostat instead of liquid helium. This is feasible due to its triple point of 161.4 K, whereas typical Helium-3 porous media studies require a much lower temperature range of $1.5 - 3.15$ K.

The aim of this paper is to demonstrate the potential of ^{129}Xe NMR for investigating porous media at temperatures near the triple point of Xenon. Xenon gas (produced by Production and Trading Company "Kriogen", Ekaterinburg, Russia, 99.9998% purity) with natural isotopic composition and Boltzmann polarization was used in the experiments.

2. Experimental setup

Experiments were performed using the home-built pulse NMR spectrometer with digital quadrature detection equipped with a helium/nitrogen cryostat (LH-311-1.5K-MRI), operating in the temperature range from 1.5 to 325 K, and a resistive magnet. This spectrometer allows to perform experiments in the magnetic fields from 0 to 0.85 T and at NMR frequencies from 3 to 150 MHz, covering a wide range of NMR experiments on various nuclei. A diagram of the main elements of an NMR setup with gas communication and simplified block diagram of the pulse NMR spectrometer are presented in Figure 1. A more detailed description of the NMR spectrometer can be found in references [14, 15]. For signal detection, a preamplifier with a gain of 64 dB and a bandwidth of 1 MHz to 500 MHz was used.

Prior to experiments, gaseous Xenon was purified using a method similar to that described in reference [16]. A volume (V_{gas}, Figure 1), initially filled with gaseous Xenon, was immersed in liquid nitrogen. After the Xenon had frozen (solidified) and the pressure in the volume had dropped to a few mbar (monitored by manometer M1 in Figure 1; the vapor pressure of Xe at 77 K is ca. 3 mTorr [12]), the pumping by a turbomolecular pump was turned on for 10–15 minutes. Subsequently, the pumping valve was closed, the Xenon-containing volume was warmed

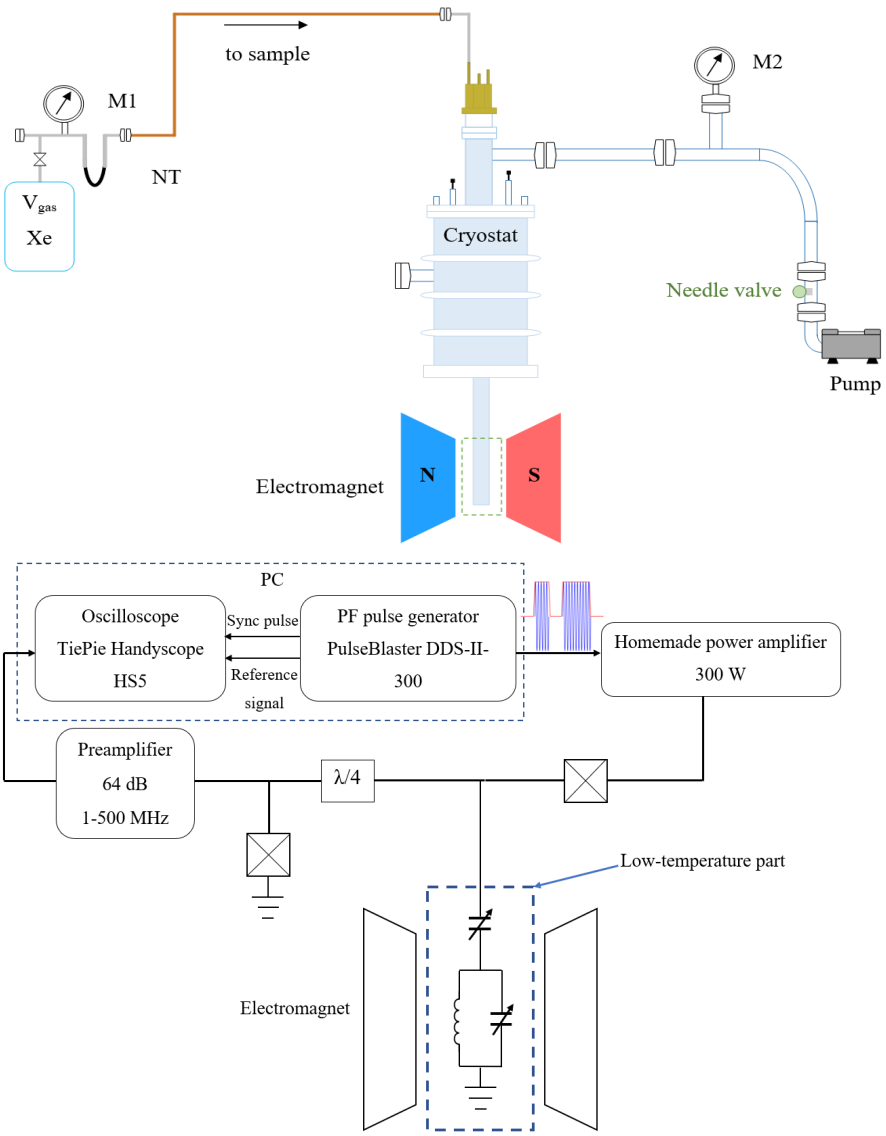

Figure 1. Diagram of the main elements of NMR setup (V_{gas} – gas storage volume, M1/M2 – manometer, NT – liquid nitrogen trap) (top) and block diagram of the NMR spectrometer (bottom).

up, and the freeze-pump-thaw cycle was repeated several times. Additionally, before conducting experiments, all gas lines connected to the sample were evacuated using a turbomolecular pump and then further pumped using a liquid nitrogen trap (NT, Figure 1) for 12-15 hours.

The inherent *sensitivity* of the proposed method is low, as observing Xe-129 NMR using Xenon with natural isotopic abundance (26.4% for ^{129}Xe) and Boltzmann polarization is challenging. Using liquid Xenon near its triple point temperature (161.4 K) enhances the NMR signal by approximately a factor of 1000 compared to gaseous Xenon at STP. Due to the low gyromagnetic ratio of ^{129}Xe ($\gamma/2\pi = -11.78$ MHz/T) and the use of a resistive magnet, a significant increase in the sensitivity of the NMR spectrometer was required.

The Xenon *phase diagram and the difficulties associated with condensing* Xenon into the experimental cell also warrant careful consideration. Initial experiments highlighted the critical *importance of reliable temperature gradient control* along the NMR probe axis. Consequently, five thermometers and two heaters were installed. However, the installation of these elements introduced *additional RF-noise from the electrical leads.*

3. Solutions implemented

For sensitivity increasing a low-temperature, high-Q NMR probe (Figure 2) with a variable frequency was developed and assembled. Tuning and matching of the LC-circuit were achieved by using two low-temperature variable capacitors. The typical dimensions of the NMR coils used in this study were: length $L = 20\,\text{mm}$ and diameter $d = 8\,\text{mm}$. The number of turns was 27 for ^{3}He NMR and approximately 60 for ^{129}Xe NMR.

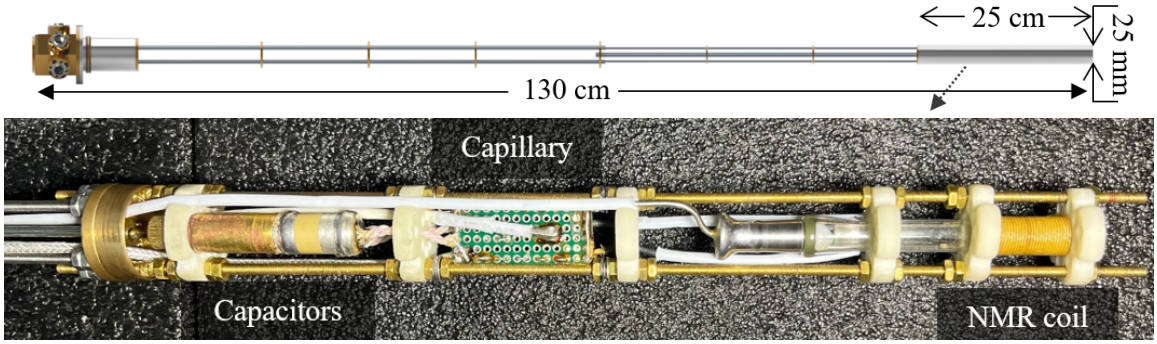

Figure 2. Model of the NMR probe (top) and a photo of the realized NMR cell, detailing the arrangement of the capillary, NMR coil, and capacitors (bottom).

To evaluate the sensitivity of the NMR spectrometer equipped by the developed probe, a gaseous mixture of ^{3}He and ^{4}He (80% ^{3}He concentration) was introduced into the experimental cell (inner diameter of the ampoule is 6 mm) at a pressure of 600 mbar and a temperature of $T = 100\,\text{K}$. An inverse opal SiO_2 sample with a pore size of $224 \pm 15\,\text{nm}$, consisting of irregularly shaped particles ($1 - 3\,\text{mm}$), was selected as a test sample (Figure 3).

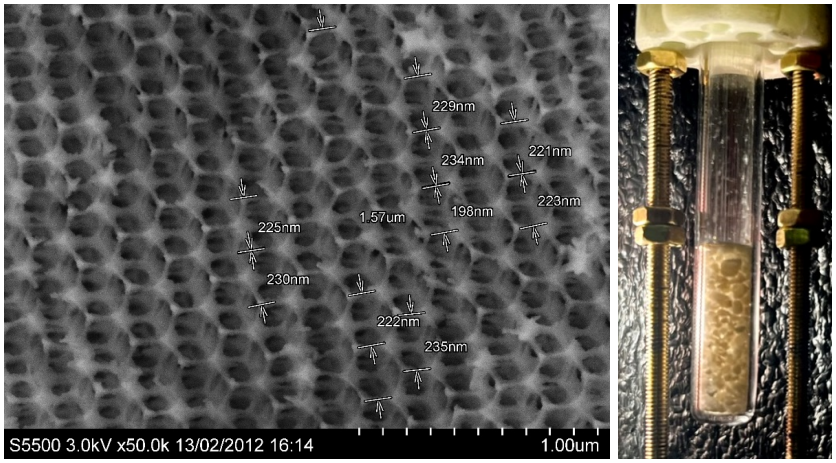

Figure 3. Inverse opal SiO_2 sample and its loading into an NMR cell

A two-pulse spin-echo sequence $(\frac{\pi}{2} - \tau - \pi)$ was used to observe the spin echo signal. The spin-lattice relaxation time T_1 was studied using the sequence: $\frac{\pi}{2}(saturation\ pulse) - t - \frac{\pi}{2} - \tau - \pi$. Figure 4 shows the longitudinal magnetization recovery curve of ^{3}He nuclei in the sample, obtained with 64 averages and the following pulse sequence parameters: $15\,\mu\text{s}\,(15\%)$ – $t\,(20\,\text{ms} - 10\,\text{s})$ – $15\,\mu\text{s}\,(15\%)$ – $1000\,\mu\text{s}$ – $15\,\mu\text{s}\,(20\%)$ (transmitter power percentage is indicated in brackets). The data were fitted with a single-exponential function, yielding $T_1 = 788.8 \pm 73.2\,\text{ms}$. After determining the time for full longitudinal magnetization recovery, spin echo signals were recorded using the sequence: $15\,\mu\text{s}\,(15\%)$ – $1000\,\mu\text{s}$ – $15\,\mu\text{s}\,(20\%)$. The resulting spin echo signal

(128 averages, sequence repetition time 3000 ms) in the time domain is shown in Figure 4.

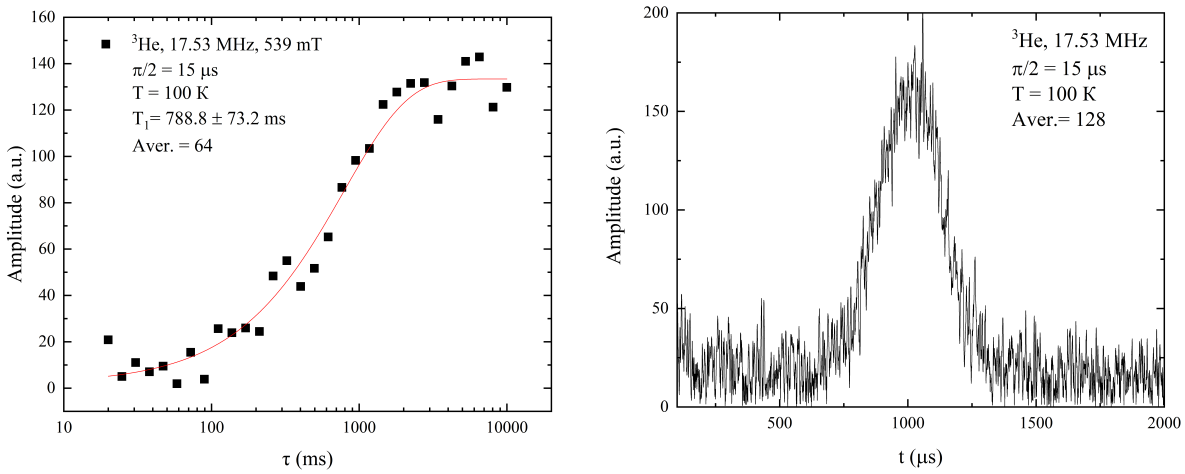

Figure 4. Recovery of longitudinal magnetization of gaseous ^{3}He nuclei in an inverse opal sample at $T = 100$ K (left). Spin echo signal of gaseous ^{3}He after 128 averages in an inverse opal sample at $T = 100$ K (right).

These measurements confirmed the achieved minimal sensitivity required for observing the ^{129}Xe NMR signal and the functionality of the LC-circuit tuning and matching. A detailed description of the probe assembly will be published elsewhere.

Special attention must be paid to the Xenon phase diagram (shown in Figure 5). Thus, at the triple point, the saturated vapor pressure is $P_{\mathrm{TP}} = 816$ mbar and the temperature is $T_{\mathrm{TP}} = 161.4$ K [17], while at the boiling point: $P = 1000$ mbar, $T = 165$ K [17]. This implies that experiments with the liquid phase at normal pressure are confined to a narrow temperature window of 3.6 K. Furthermore, the transition of Xenon from the liquid to the solid phase is not accompanied by an abrupt drop of saturated vapor pressure.

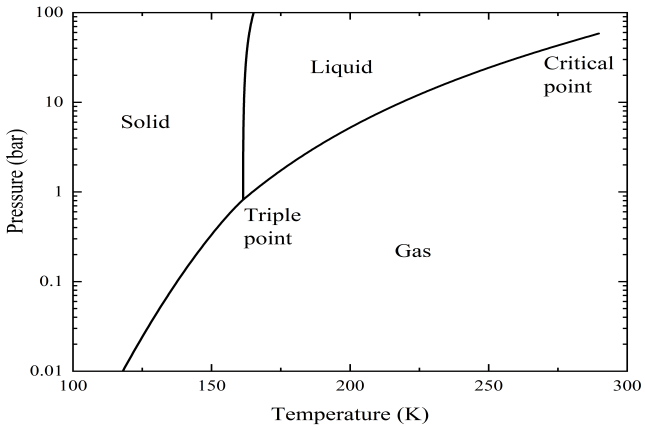

Figure 5. Phase diagram of Xenon. Redrawn from [18].

Condensing Xenon into the experimental cell requires pre-cooling the cell down to 100-120 K. Under these conditions, Xenon condenses directly into the solid phase, which subsequently must be melted into the liquid state. During initial testing of this procedure, capillary blockage occurred. Intensive purging with a high flow of gaseous nitrogen through the cryostat can create cold spots where Xenon freezes on the capillary walls. To prevent this in following experiments, a heater was wound on the capillary. To accurately control the heater power and the temperature

gradient along the NMR probe axis, five Pt1000 thermometers were installed. For precise control of the Xenon phase inside the experimental cell, another heater was installed at the bottom of the probe to additionally heat the gas flow. Figure 6 shows schematic diagram of the NMR cell cooled by nitrogen gas flow.

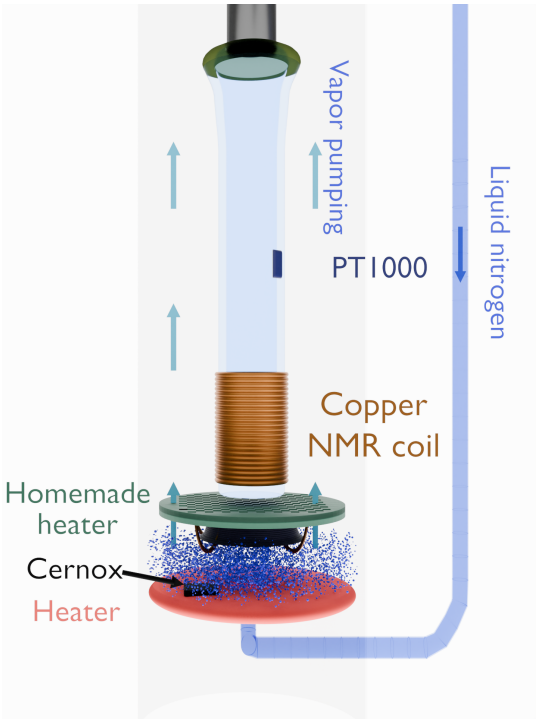

Figure 6. Cooling the NMR cell by nitrogen gas flow. The diagram also shows the position of the homemade heater and a Pt1000 thermometer.

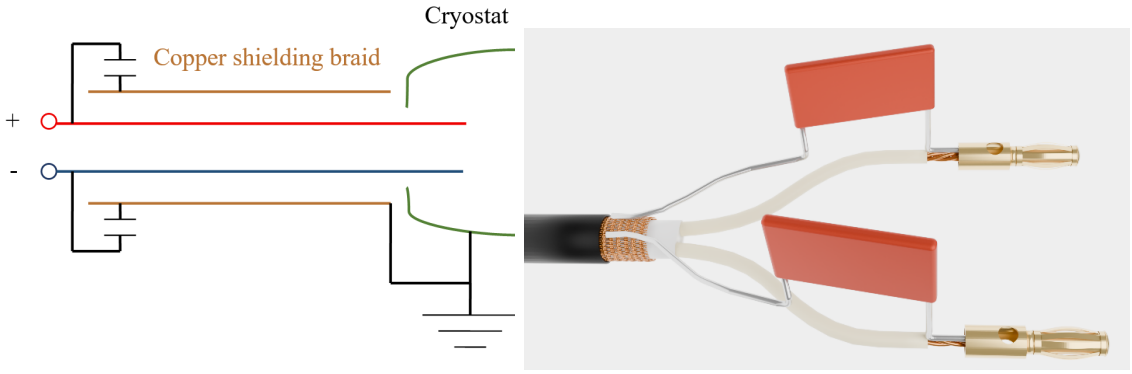

Figure 7. Shielding diagram for heater leads: wires are placed within a copper shielding braid, and power filters (ceramic capacitors of 10 and 100 nF in parallel connection) are added.

The addition of multiple leads for heaters and thermometry, some in close proximity to the NMR cell, resulted in a significant degradation of sensitivity and an increase in RF-noise (by more than a factor of 100). To resolve this, several measures were implemented: the RF-ground outside the cryostat was improved, external leads were shielded with a copper braid, power supply filters were added (Figure 7), and the heater located near the NMR cell was isolated from the NMR coil by using a grounded copper mesh. These steps restored the sensitivity almost to the level prior to the installation of the heaters and thermometry.

Only after addressing these challenges it was possible to achieve controlled condensation of Xenon into the experimental cell. The following procedure for filling the NMR cell with liquid Xenon was developed and tested:

1. Pre-cooling the NMR cell down to 190 K,
2. Turning on the capillary heater to prevent blockage,
3. Opening the valve (Figure 1) and connecting the Xe-containing volume to the cell,
4. Cooling the cell down to 100 K,
5. Shutting off the valve, separating the Xe-containing volume,
6. Warming up the NMR cell with Xe, turning on the bottom heater, and following the melting curve (Figure 5),
7. Stabilizing the temperature.

The entire procedure takes about two hours.

4. Results and Discussion

Given inconsistencies in published data on the NMR relaxation times of liquid Xenon, purified Xenon with natural isotopic abundance and Boltzmann polarization was investigated. Figure 8 shows the spin echo signal in the time domain and the spin-lattice relaxation curve of bulk liquid ^{129}Xe, obtained by a single scan at a frequency of $f_0 = 9.06$ MHz and at a temperature of $T = 164.4$ K (the temperature corresponding to the saturated vapor pressure, monitored by manometer M1 in Figure 1). The spin echo was observed using a two-pulse sequence: $\frac{\pi}{2}_x - \tau - \pi_y$, where $\frac{\pi}{2} = 12\,\mu$s, $\pi = 24\,\mu$s, $\tau = 2000\,\mu$s. The spin-lattice relaxation time T_1 was measured using the sequence: $\frac{\pi}{2}_x$ (saturation pulse) $- t - \frac{\pi}{2}_x - \tau - \pi_y$, where $\frac{\pi}{2} = 12\,\mu$s, $\pi = 24\,\mu$s, $\tau = 2000\,\mu$s, t varied from 10 s to 10000 s.

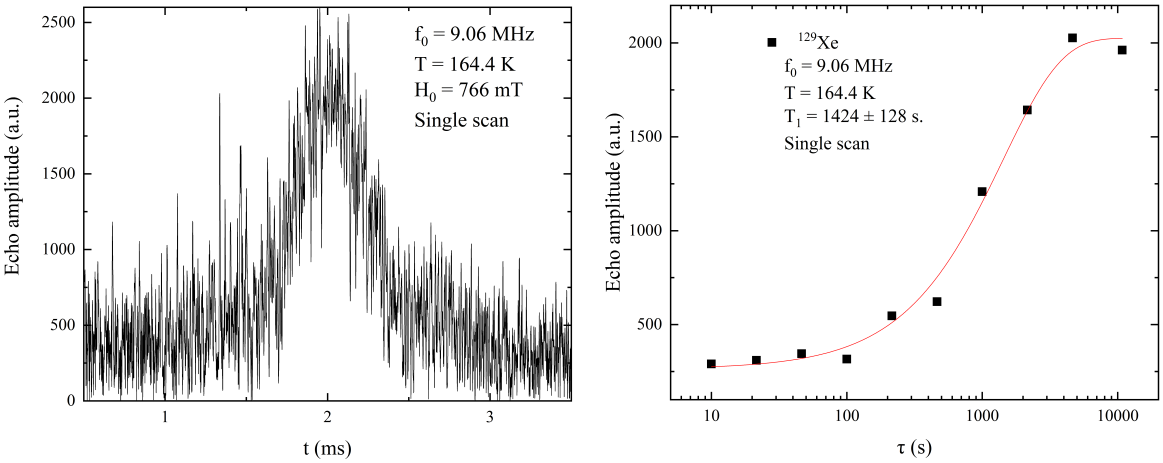

Figure 8. Spin echo signal (left) and spin-lattice relaxation curve (right) of bulk liquid ^{129}Xe at a frequency of 9.06 MHz at a temperature of $T = 164.4$ K, obtained by a single scan.

The measured spin-lattice relaxation time was $T_1 = 1424 \pm 128$ s. (≈ 23.7 min.). Due to long relaxation time, signal averaging was not performed. Hunt and Carr [19] earlier investigated

relaxation in thermally polarized liquid ^{129}Xe, reporting $T_1 = 16.5 \pm 3$ min. at $T = 201$ K. Furthermore, Sauer et al. [20] studied hyperpolarized liquid Xenon at different temperatures, magnetic fields, and cell surfaces. They observed relaxation times exceeding 30 minutes near the triple point and reported T_1 values at 200 K of 20.5 ± 0.4 min. in the earth's magnetic field (0.05 mT); 25.1 ± 0.3 min. and 24.5 ± 0.4 min. in a 1.4 T field.

Additionally, the spin-spin relaxation time T_2 was estimated using the Car-Purcell-Meiboom-Gill (CPMG) sequence. Limited by instrumental constraints (which also require further refinement in the future), the result was $T_{2\mathrm{CPMG}} > 20$ s. Yen and Norberg [21] studied the temperature dependence of the spin-spin relaxation time T_2 of ^{129}Xe in the liquid and solid phases using the Carr-Purcell-Meiboom pulse sequence, however, their samples were intentionally contaminated with a small amount of oxygen to reduce the spin-lattice relaxation time. They reported $T_2 \approx 7$ s. in the triple point region for liquid Xenon at a frequency of 10.5 MHz in an 892 mT field.

Experiments were also carried out to observe the relaxation times of Xenon in the solid phase at 160.5 K, yielding a spin-lattice relaxation time $T_1 = 511 \pm 35$ s. and an estimated spin-spin relaxation time $T_{2\mathrm{CPMG}} \sim 9$ s. Surprisingly, the values obtained for solid Xenon are significantly lower than those for liquid Xenon. This will be the subject of future investigation.

To test the capability of the ^{129}Xe NMR method for probing porous media, the same sample used for the sensitivity test (Figure 3) was used. Changes in the NMR characteristics of ^{129}Xe were confirmed upon introducing the sample into the NMR cell: the relaxation times became shorter compared to those of bulk Xenon, and a biexponential decay was evident in the T_2 relaxation curve measured by the CPMG method. Figure 9 illustrates two $T_{2\mathrm{CPMG}}$ relaxation

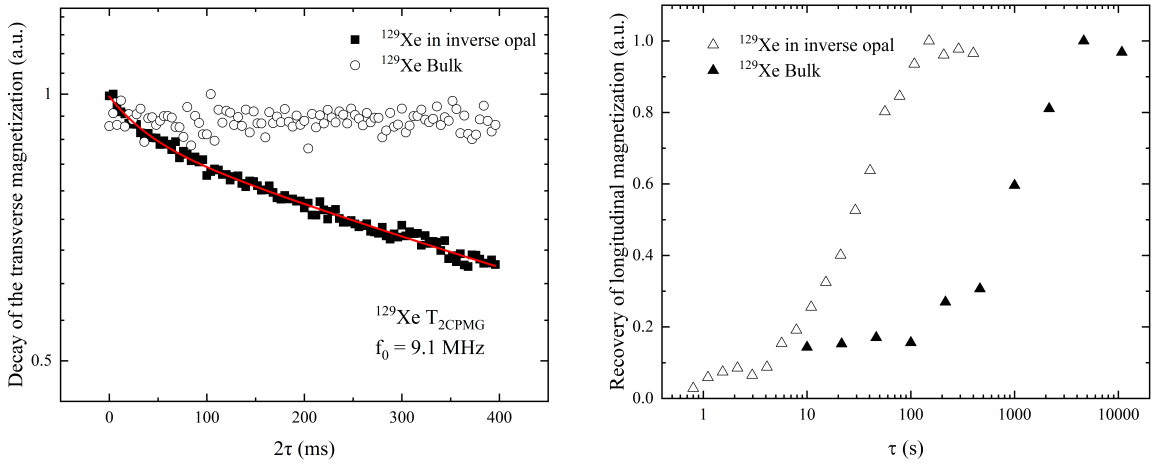

Figure 9. Comparison of the decay of the transverse magnetization (left) and the recovery of longitudinal magnetization (right) of liquid ^{129}Xe in bulk Xenon and in an inverse opal sample at a temperature of $T = 164.4$ K.

curves of liquid ^{129}Xe in bulk Xenon and within the sample, alongside the change in the spin-lattice relaxation time of ^{129}Xe in the sample. The obtained T_1 relaxation times were significantly shorter, ranging from 38 to 70 s at different temperatures. However, definitive values for the relaxation times of Xenon in this porous medium and their interpretation are not provided here, as the probable issue of sample flotation in liquid Xenon (due to the density difference) seems to be emerged.

5. Conclusions

In this study, bulk Xenon was investigated and preliminary results for Xenon in a porous medium at temperatures near the triple point of Xenon were obtained. The values of the spin-lattice relaxation time in the liquid ($T_1 = 1424 \pm 128$ s.) and solid ($T_1 = 511 \pm 35$ s.) phases were obtained. The spin-spin relaxation times were estimated for the liquid ($T_2 > 20$ s) and solid ($T_2 \sim 9$ s) phases. The measured spin-lattice and spin-spin relaxation times for bulk Xenon are consistent with literature data, indicating high gas purity and the validity of the purification procedure. The proposed ^{129}Xe NMR method has proven viable and sensitive to the presence of porous media, as evidenced by shortened relaxation times and biexponential behavior in the $T_{2\text{CPMG}}$ relaxation curve compared to bulk Xenon. However, obtaining the first signal and preliminary results with the sample required overcoming numerous technical problems. Following further instrumental improvements, experiments are planned with samples of varying porosity, aiming to develop a characterization methodology based on ^{129}Xe NMR near triple point temperatures.

Acknowledgments

This work was financially supported by the subsidy of Ministry of Science and Higher Education of the Russian Federation to Kazan Federal University (FZSM-2023-0012).

References

1. Boventi M., Mauri M., Simonutti R. *Applied Sciences* **12**, 3152 (2022).
2. Stanislavovas A., Kuzmin V., Safiullin K., Alakshin E., Klochkov A., Kutuzov M., Tagirov M. *Journal of Physics: Condensed Matter* **33**, 195805 (2021).
3. Kuzmin V., Safiullin K., Dolgorukov G., Stanislavovas A., Alakshin E., Safin T., Yavkin B., Orlinskii S., Kiiamov A., Presnyakov M., Tagirov M. *Physical Chemistry Chemical Physics* **20**, 1476 (2018).
4. Safiullin K., Kuzmin V., Bogaychuk A., Alakshin E., González L., Kondratyeva E., Dolgorukov G., Gafurov M., Klochkov A., Tagirov M. *Journal of Petroleum Science and Engineering* **210**, 110010 (2022).
5. Gazizulin R. R., Klochkov A. V., Kuzmin V. V., Safiullin K. R.,Tagirov M. S., Yudin A. N., Izotov V. G., Sitdikova L. M. *Applied Magnetic Resonance* **38**, 271 (2010).
6. Proctor W. G., Yu F. C. *Physical Review* **78**, 471 (1950).
7. Proctor W. G., Yu F. C. *Physical Review* **81**, 20 (1951).
8. Ito T., Fraissard J. *The Journal of Chemical Physics* **76**, 5225 (1982).
9. Raftery D., Long H., Meersmann T., Grandinetti P. J., Reven L., Pines A. *Physical Review Letters* **66**, 584 (1991).
10. Wisser D., Hartmann M. *Advanced Materials Interfaces* **8**, 2001266 (2021).
11. Weiland E., Springuel-Huet M. A., Nossov A., Gedeon A. *Advanced Materials Interfaces* **225**, 41 (2016).
12. Cho G., Moran L. B., Yesinowski J. P. *Applied Magnetic Resonance* **8**, 549 (1995).
13. Li L., Guo L., Zhang Z., Yang Q., Yang Y., Bao Z., Ren Q., Li J. *Journal of the American Chemical Society* **141**, 9358 (2019).

14. Alakshin E. M., Gazizulin R. R., Klochkov A. V., Kuzmin V. V., Sabitova A. M., Safin T. R., Tagirov M. S. *Magnetic Resonance in Solids. Electronic Journal* **15**, 13104 (2013).
15. Dolgorukov G. A., Kuzmin V. V., Bogaychuk A. V., Alakshin E. M., Safiullin K. R., Klochkov A. V., Tagirov M. S. *Magnetic Resonance in Solids. Electronic Journal* **20**, 18206 (2018).
16. Moudrakovski I. L., Breeze S. R., Simard B., Ratcliffe C. I., Ripmeester J. A., Seideman T., Tse J. S., Santyr G. *The Journal of Chemical Physics* **114**, 2173 (2001).
17. Xenon - the NIST WebBook.
18. Cherubini A., Bifone A. *Progress in Nuclear Magnetic Resonance Spectroscopy* **42**, 1 (2003).
19. Hunt E. R., Carr H. Y. *Physical Review* **130**, 2302 (1963).
20. Sauer K. L., Fitzgerald R. J., Happer W. *Chemical physics letters* **277**, 153 (1997).
21. Yen W. M., Norberg R. E. *Physical Review* **131**, 269 (1963).